An efficient reliability analysis method for structures with hybrid time-dependent uncertainty

Kun Zhang[1], Ning Chen[1,*], Peng Zeng[1], Jian Liu[1], Michael Beer[2,3,4]

[1]State Key Laboratory of Advanced Design and Manufacturing for Vehicle Body, Hunan University, Changsha 410082, China

[2]Institute for Risk and Reliability, Leibniz Universität Hannover, Callinstr. 34, Hannover, Germany

[3]Institute for Risk and Uncertainty, University of Liverpool, Peach Street, L69 7ZF Liverpool, United Kingdom

[4]International Joint Research Center for Resilient Infrastructure & International Joint Research Center for Engineering Reliability and Stochastic Mechanics, Tongji University, Shanghai, China

Abstract: Performing time-dependent reliability analysis is an effective way to estimate the failure probability of structural system throughout its lifetime. In the engineering practices, uncertain parameters with sufficient sample and limited sample may exist simultaneously. The uncertain parameters with limited sample data are difficult to construct its precise probabilistic characteristics during estimating the accurate time-dependent reliability. To address this issue, this paper first develops a new hybrid time-dependent reliability model involving interval processes. Then, to reduce the high dimensionality, an extension method based on equivalent stochastic process transformation approach is proposed to transform the stochastic processes and the interval processes into corresponding equivalent random variables respectively. In particular, an instantaneous reliability model is constructed to envelope all potential system failures that may occur during the time interval. In order to identify the instantaneous failure surface accurately, an active learning method is proposed based on the deep neural network model and the weighted sampling method. With the constructed deep neural network model, the new hybrid time-dependent reliability can

Fax number of the corresponding author: 0731-88822825

E-mail address of the corresponding author: chenning@hnu.edu.cn (N. Chen)

be evaluated by performing the Monte Carlo Sampling. Three numerical examples are used to verify the accuracy and efficiency of the proposed method.

Keywords: Time-dependent reliability analysis, Deep neural network, Active learning, Weighted sampling, Hybrid uncertain model

1. Introduction

Considering the ubiquitous uncertain factors, the structural reliability analysis is used to determine the failure probabilities of structures. In general, uncertainty can be classified into two types: aleatory and epistemic [1]. Aleatory uncertainty is caused by the inherent variations of an objective physical system and will not be reduced with the increase of cognitive level. Many methods can be used to handle the aleatory uncertainty [2-5]. However, epistemic uncertainty is caused by the limitation of subjective cognitive level and will be reducible by additional empirical information. Epistemic uncertainty models include fuzzy sets [6], probability box [7, 8], interval model [9] and so forth. In these researches, the time-varying effect is not taken into account.

However, in view of the structural performance degeneration, stochastic operation conditions and time-dependent load processes [10, 11], traditional static reliability methods may not be feasible any more. In order to tackle the time-varying effect, two main types of time-variant reliability methods have been developed [12]. They are the outcrossing rate-based methods and the extreme value-based methods. The core of outcrossing rate-based methods is to obtain the time-dependent reliability by calculating and then integrating the outcrossing rate. The outcrossing event occurs when the response reaches the limit state and the outcrossing rate is defined as the change rate of the outcrossing probability with respect to time. To address more general time-dependent reliability problem, Andrieu-Renaud et al. proposed the PHI2 method to estimate the outcrossing rate by using time-invariant parallel system approach [13]. Hu and Du extended the existing joint outcrossing rate method to the general limit-state functions with both random variables and stochastic processes [14]. Even though

outcrossing rate-based methods have developed greatly over the past decades, they are still inaccurate for nonlinear and multimodal problems due to their inherent defects such as the embedded first-order reliability method (FORM) and the low resolution of discretized time dimension.

In extreme value-based methods, the failure probability is evaluated based on the worst performance of an engineering system within a time interval. A failure occurs if the system does not satisfy its requirements when subjected to the extreme values. Xu et al. proposed a new method to obtain the extreme value distribution by employing the maximum entropy method with fractional moments as constraints, where an adaptive cubature formula is utilized for fractional moments assessment [15]. By obtaining the extreme value distribution, a time-dependent reliability problem can be transformed into a time-independent case, and then conventional reliability analysis methods can be applied. However, it is usually intractable to obtain the probabilistic characterization of the extreme value analytically in practical problems. Though simulation-based methods can be used to estimate the extreme value distribution, the required computational resources are still significant due to the inevitable large number of function evaluations. To overcome the inefficiency of the simulation-based methods, surrogate models, such as polynomial chaos expansion [16, 17], Kriging [18-20], and artificial neural networks [21-23] are employed to replace the performance functions for reducing the computational burden. The active learning strategy can further improve the efficiency of the approaches using surrogate models. Xiang et.al proposed an active learning method for structural reliability analyses by combining the deep neural network (DNN) model and the weighted sampling method [24], which can be termed as WS-DNN. Shi et.al developed an active learning reliability method with multiple kernel functions based on radial basis function (CVRBF-MCS) [25].

However, all of these methods mentioned above are only capable of performing time-dependent analysis when there is sufficient information to construct precise probabilistic characteristics of uncertain parameters. They cannot handle the cases that

uncertain parameters lack of sample data. Under this circumstance, Wang et al. and Jiang et al. proposed the non-probabilistic interval process and the non-probabilistic convex process model for analyzing the time-dependent reliability of the mechanisms respectively [26, 27]. Chang et al. developed a new non-probabilistic time-dependent reliability model for the input interval uncertainties [28]. Wang et al. proposed a novel convexity-oriented time-dependent reliability-based topology optimization framework, where the nodal dynamic responses are expressed by the convex process model [29].

In the engineering practices, uncertain parameters with sufficient sample data and limited sample data may exist simultaneously. Although many researchers have intensively investigated the hybrid reliability analysis with both random and interval uncertainties to handle this situation [30-33], the time-varying effect is not taken into account. The difficulty of time-dependent reliability analysis will see a remarkable increase when both the random uncertainties and the interval uncertainties are involved. So far, the researches on the hybrid time-dependent reliability analysis have been rarely performed. Wang et al. proposed a method based on projection outline adaptive Kriging (POK) to handle time-dependent reliability analysis with mixed interval uncertainties (iTRA) [34]. For analyzing the reliability of the dynamic structure involving both input random variables and the interval ones, Shi et al. presented a new dynamic reliability analysis model and established a double-loop optimization algorithm based on the active learning Kriging method [35]. To the best of our knowledge, the study on reliability analysis considering both stochastic processes and interval processes is not conducted. Under this circumstance, a new hybrid time-dependent reliability model involving interval processes (HTR-ip) is first developed here. Furthermore, it is essential and urgent to seek a simple, efficient and practical time-dependent reliability analysis method for the developed new time-dependent hybrid reliability model.

In this paper, an efficient approach for the new hybrid time-dependent reliability analysis is proposed by combining equivalent uncertainty transformation and active learning. In the proposed method, an extension method based on the equivalent

stochastic process transformation approach (eSPT) [36] is introduced firstly to transform the stochastic processes and the interval processes into corresponding equivalent random variables, which can be used for constructing the instantaneous reliability model. Based on the limit state function and exact equivalent uncertainty transformation, the instantaneous reliability model possesses the capability of identifying all potential instantaneous failure events for predicting time-variant failures. Then aiming at the transformed static reliability analysis, an active learning method based on the DNN and weighted sampling is proposed to accurately identify the instantaneous failure surface. Finally, the time-variant reliability can be obtained approximately using the MCS samples and the constructed DNN surrogate model.

The rest of this paper is organized as follows. Section 2 provides a brief introduction about the new hybrid time-dependent reliability model involving interval processes. Section 3 introduces the details of the proposed computational method for the new hybrid time-dependent reliability model. The computational efficiency and accuracy of proposed method is demonstrated with three examples in Section 4. Section 5 provides some conclusions.

2. Definition of the new hybrid time-dependent reliability model involving interval processes (HTR-ip)

2.1 Fundamentals of interval process

In this paper, the interval process is introduced to express the uncertainty of time-variant process with limited data. Based on the interval variable characteristics and the extension of the classic stochastic process theory, several important characteristics about interval process will be introduced.

Definition 1. For an interval process $I(t)$ with the lower bound $I^L(t)$ and the upper bound $I^U(t)$, the middle point function $I^M(t)$ and the radius function $I^R(t)$ can be defined as:

$$I^M(t) = \frac{I^U(t)+I^L(t)}{2} \tag{1}$$

$$I^R(t) = \frac{I^U(t) - I^L(t)}{2} \tag{2}$$

Definition 2. For an interval process $I(t)$, the auto-correlation coefficient function of interval variables $I(t_i)$ and $I(t_j)$ at any two time instants t_i and t_j is defined as:

$$\rho_{II}(t_i, t_j) = \frac{Cov_{II}(t_i, t_j)}{\sqrt{D_I(t_i)}\sqrt{D_I(t_j)}} \tag{3}$$

where $Cov_{II}(t_i, t_j)$ is the auto-covariance function of interval variables $I(t_i)$ and $I(t_j)$, $D_I(t)$ is the variance function. In this work, assuming that $\rho_{II}(t_i, t_j)$ is an exponential correlation function, Eq. (3) can be rewritten as:

$$\rho_{II}(t_i, t_j) = \exp(-\frac{|t_i - t_j|}{l}) \tag{4}$$

where l is called correlation length. More details about interval process theory can refer to reference [27].

2.2 Implementation of HTR-ip based on Monte Carlo simulation method

In the time-variant reliability problem, uncertain parameters with sufficient sample data and limited sample data may exist simultaneously. Here, a new hybrid time-dependent reliability analysis model involving interval processes (HTR-ip) is constructed to provide an alternative path to deal with this kind of problem. Its limit state function can be expressed as

$$G = g(\boldsymbol{X}, \boldsymbol{Y}, \boldsymbol{S}(t), \boldsymbol{I}(t), t) \tag{5}$$

where $\boldsymbol{X} = (X_1, X_2, \dots X_m)$ indicates the m-dimensional vector of the random variables and $\boldsymbol{Y} = (Y_1, Y_2, \dots Y_n)$ indicates the n-dimensional vector of the interval variables. $\boldsymbol{S}(t) = [S_1(t), S_2(t), \dots S_p(t)]$ is a vector of p stochastic processes input and $\boldsymbol{I}(t) = [I_1(t), I_2(t), \dots I_l(t)]$ is a vector of l interval processes input. It is noted that the variables in the limit state function are independent of each other.

Given a specified time period $[0, T_L]$, for the hybrid time-dependent uncertain limit state function $g(\boldsymbol{X}, \boldsymbol{Y}, \boldsymbol{S}(t), \boldsymbol{I}(t), t)$ with mixed stochastic and interval processes, the failure probability over a time interval $[0, T] (0 \le T \le T_L)$ can be defined as follows

$$P_f(0,T) = Prob\left\{\begin{matrix} g(\boldsymbol{X},\boldsymbol{Y},\boldsymbol{S}(t),\boldsymbol{I}(t),t) \le 0, \\ \exists t \in [0,T], \boldsymbol{Y} \in [\boldsymbol{Y}^L,\boldsymbol{Y}^U], \boldsymbol{I}(t) \in [\boldsymbol{I}^L(t),\boldsymbol{I}^U(t)] \end{matrix}\right\}, \quad 0 \le T \le T_L \quad (6)$$

Owing to the time-dependency of system failures, it is technically intractable to derive a closed-form solution for calculating time-variant probability of failure in Eq. (6). Therefore, the extreme value-based methods are used to approximate the failure probability. Furthermore, considering the existence of interval variables and interval processes, the failure probability should be located in an interval $[P_f^{min}, P_f^{max}]$. Its lower and upper bounds can be formulated as

$$P_f^{min} = prob\left\{\min_{t\in[0,T]}\left(\max_{\boldsymbol{Y}\in[\boldsymbol{Y}^L,\boldsymbol{Y}^U],\boldsymbol{I}(t)\in[\boldsymbol{I}^L(t),\boldsymbol{I}^U(t)]} g(\boldsymbol{X},\boldsymbol{Y},\boldsymbol{S}(t),\boldsymbol{I}(t),t)\right) \le 0\right\} \quad (7)$$

$$P_f^{max} = prob\left\{\min_{t\in[0,T]}\left(\min_{\boldsymbol{Y}\in[\boldsymbol{Y}^L,\boldsymbol{Y}^U],\boldsymbol{I}(t)\in[\boldsymbol{I}^L(t),\boldsymbol{I}^U(t)]} g(\boldsymbol{X},\boldsymbol{Y},\boldsymbol{S}(t),\boldsymbol{I}(t),t)\right) \le 0\right\} \quad (8)$$

The MCS method can be used for evaluating the failure probability defined in Eqs. (7)-(8). In the MCS method, N random realizations of the input variables $\boldsymbol{V_o}$ are generated. The i th random input variables can be denoted as $\boldsymbol{V_o}^i = [\boldsymbol{X}^i, \boldsymbol{Y}, \boldsymbol{S}^i(t), \boldsymbol{I}(t), t]$. Then the failure probability can be calculated by

$$P_f^{min} \approx \sum_i^N I_{min}(\boldsymbol{V_o}^i)/N \quad (9)$$

$$P_f^{max} \approx \sum_i^N I_{max}(\boldsymbol{V_o}^i)/N \quad (10)$$

where $I_{min}(\boldsymbol{V_o}^i)$ and $I_{max}(\boldsymbol{V_o}^i)$ represents the failure indicator functions of ith random input parameters $\boldsymbol{V_o}$, which can be given as Eqs. (11)-(12).

$$I_{min}(\boldsymbol{V_o}^i) = \begin{cases} 1 & \min\limits_{t\in[0,T]}\left\{\max\limits_{\boldsymbol{Y}\in[\boldsymbol{Y}^L,\boldsymbol{Y}^U],\boldsymbol{I}(t)\in[\boldsymbol{I}^L(t),\boldsymbol{I}^U(t)]} g(\boldsymbol{X}^i,\boldsymbol{Y},\boldsymbol{S}^i(t),\boldsymbol{I}(t),t)\right\} \le 0 \\ 0 & \min\limits_{t\in[0,T]}\left\{\max\limits_{\boldsymbol{Y}\in[\boldsymbol{Y}^L,\boldsymbol{Y}^U],\boldsymbol{I}(t)\in[\boldsymbol{I}^L(t),\boldsymbol{I}^U(t)]} g(\boldsymbol{X}^i,\boldsymbol{Y},\boldsymbol{S}^i(t),\boldsymbol{I}(t),t)\right\} > 0 \end{cases},$$

$$\forall i = 1,2,\dots,N \quad (11)$$

$$I_{max}(\boldsymbol{V_o}^i) = \begin{cases} 1 & \min\limits_{t\in[0,T]}\left\{\min\limits_{\boldsymbol{Y}\in[\boldsymbol{Y}^L,\boldsymbol{Y}^U],\boldsymbol{I}(t)\in[\boldsymbol{I}^L(t),\boldsymbol{I}^U(t)]} g(\boldsymbol{X}^i,\boldsymbol{Y},\boldsymbol{S}^i(t),\boldsymbol{I}(t),t)\right\} \le 0 \\ 0 & \min\limits_{t\in[0,T]}\left\{\min\limits_{\boldsymbol{Y}\in[\boldsymbol{Y}^L,\boldsymbol{Y}^U],\boldsymbol{I}(t)\in[\boldsymbol{I}^L(t),\boldsymbol{I}^U(t)]} g(\boldsymbol{X}^i,\boldsymbol{Y},\boldsymbol{S}^i(t),\boldsymbol{I}(t),t)\right\} > 0 \end{cases},$$

$$\forall i = 1,2,\dots,N \quad (12)$$

Different from traditional static reliability methods, the most challenging part is to

calculate reliability level of an engineered system high efficiently yet accurately during its life cycle. To improve computational efficiency, the surrogate model methods can be employed to replace the performance function and reduce the computational burden.

3. The proposed reliability analysis method for HTR-ip

3.1 Equivalent uncertainty transformation

The proposed HTR-ip is essentially a time-dependent reliability problem with hybrid variables. Common operation such as transforming a time-dependent reliability problem into time-independent reliability problems at each time instants tend to fall into the dilemma of accuracy and efficiency. Inspired by eSPT, the equivalent uncertainty transformation approach (EUT) is proposed here to handle the time-variant uncertainty including both stochastic processes and interval processes. In the proposed EUT method, the time-dependent uncertainty parameters $\boldsymbol{P_t} = [\boldsymbol{S}(t), \boldsymbol{I}(t)]$ will be transformed into corresponding equivalent random variables $\boldsymbol{P_t}' = [\boldsymbol{S}', \boldsymbol{I}']$. $\boldsymbol{S}'$ is defined as the random variable transformed from the stochastic process $\boldsymbol{S}(t)$ and $\boldsymbol{I}'$ is defined as the random variable transformed from the interval process $\boldsymbol{I}(t)$. Since the instantaneous failure events at each time point have equal importance, the probability density function (PDF) of transformed random variables can be expressed as

$$f_{PDF}(\boldsymbol{P_t}') \approx \frac{1}{N}\sum_{i=1}^{N} f_{PDF}(\boldsymbol{P_t}(t_i)) \tag{13}$$

The computational cost of obtaining the probability density function of $\boldsymbol{P_t}'$ is much less than that on obtaining performance evaluations of time-dependent uncertain engineering systems, especially one can always obtain an accurate approximation of the PDF of $\boldsymbol{P_t}'$ by only increasing the number of time nodes N. For some specific cases such as Gaussian processes or stationary interval processes, analytical expression of the probability density information of $\boldsymbol{P_t}'$ can be obtained. For general cases, the random realizations of $\boldsymbol{P_t}(t)$ are generated based on spectral decomposition, and the approximate solution of the probability density information of $\boldsymbol{P_t}'$ is obtained according to Eq. (13).

The transform process of interval process is shown in Fig. 1. Compared with the stochastic process, the interval process model at any time is an interval variable, and its possible values are enclosed by an upper and a lower bound. To consider the whole potential failure events over the given time interval, the interval process can be transformed into a bounded random variable. Take a stationary interval process $I(t)$ with the middle point function $I^M(t) = 0$ and the radius function $I^R(t) = 1$ as an example. The uncertainty of interval process $I(t)$ at the ith time instant can be expressed as an interval variable $I(t_i)$ with the lower bound $I^L(t_i)$ and the upper bound $I^U(t_i)$. According to the equivalent model proposed by Jiang et.al [37], the interval variables is equivalent to independent bounded random variables following uniform distributions over their respective intervals. Therefore, the PDF of stationary interval process $I(t)$ at each time point can be expressed as

$$f_{PDF}\big(I(t_i)\big) = \begin{cases} 0 & , I(t_i) > -1 \ or \ I(t_i) < 1 \\ 0.5 & , -1 \le I(t_i) \le 1 \end{cases} \quad i \in 1,2, \dots N \tag{14}$$

Here, regardless of the number of discrete time points N, the transformed random variables I' is a bounded random variable following uniform distribution at $[-1,1]$. Furthermore, its PDF can be calculated as

$$f_{PDF}(I') = \begin{cases} 0 & , I' > -1 \ or \ I' < 1 \\ 0.5 & , -1 \le I' \le 1 \end{cases} \tag{15}$$

Once the PDF of $\boldsymbol{P_t}'$ is obtained, the time-variant reliability problem within a stochastic process and an interval process becomes the time-invariant reliability problem with random variables and bounded random variables. In addition, the parameter time t is also transformed as t'. Considering the life cycle of time-dependent engineering systems $[0, T_L]$, the t' is transformed as a parameter with uniform distribution, where $t' \sim U(0, T_L)$. For a general situation, the limit state function of hybrid time-dependent uncertain variables can be transformed as follows.

$$g(\boldsymbol{X}, \boldsymbol{Y}, \boldsymbol{S}', \boldsymbol{I}', t') \tag{16}$$

For simplicity, the transformed input parameters can be rewritten as $\boldsymbol{V_t} = [\boldsymbol{X}, \boldsymbol{Y}, \boldsymbol{S}', \boldsymbol{I}', t']$. $\boldsymbol{V_t}$ is an d-dimensional vector and $d = m + n + p + l + 1$. According

to Eq. (16), instantaneous reliability model can be constructed, which is expressed as

$$P_f = \Pr(g(\boldsymbol{V_t}) < 0) \tag{17}$$

Since the transformed limit state function $g(\boldsymbol{V_t})$ incorporates all the failure information, the hybrid time-dependent reliability analysis is converted to time-invariant counterpart. It is noted that once an accurate instantaneous reliability surrogate model is obtained, the efficiency of reliability analysis for HTR-ip will be improved. Because no matter how much the number of discrete time points adopted in MCS is, no additional DNN model is required to be trained. Furthermore, given the constructed accurate DNN model, the increased number of discrete time points used by MCS will bring additional but negligible computational consumption.

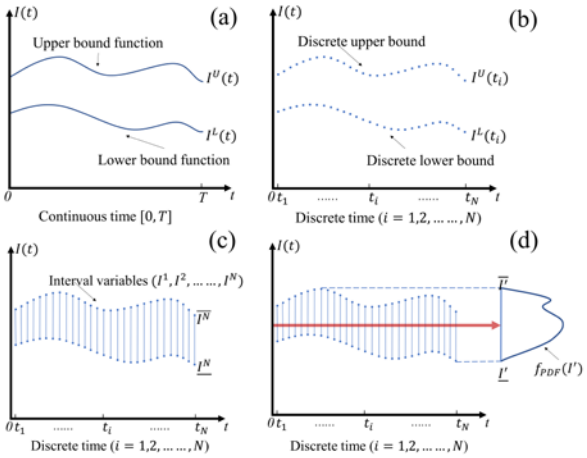

Fig. 1 The transformation process of interval process.

3.2 The proposed active learning method

3.2.1 Weighted sampling

With the constructed instantaneous reliability model as introduced above, an active learning method is proposed to calculate the probability of failure in Eq. (17) based on DNN model and weighted sampling. Before constructing the DNN surrogate model, a Monte Carlo population with N_{mc} samples is generated randomly according to the corresponding probability density function of the transformed input parameter. Then, a small number of initial training sample points are selected from the Monte Carlo population by using the weighted sampling method.

The utilized weighted sampling is designed to address the problem of uneven sampling by introducing a weighting factor that is inversely proportional to the probability of sample occurrence. Because the samples obtained by random sampling obey the probability distribution, the area with high probability in the sampling domain will contain more samples. However, it is noted that the purpose of active learning is to find the points near the limit state surface (LSS) and then use it to update the surrogate model iteratively. Considering the problem of small failure probability, the points near the LSS are always distributed in the sampling domain with a small probability. Therefore, the weighted sampling method without replacement is applied [24]. The important sample points in the population can be selected with a greater probability by giving a larger weight. In the weighted sampling method, M samples out of a population of size M_c is selected as follows:

The first and the most important step of weighted sampling is to calculate the characteristic value $c^{(i)} = \frac{\log(u^{(i)})}{w^{(i)}}$ for each item. where $w^{(i)} = \frac{1}{f(\boldsymbol{V_t}^{(i)})}$ denotes the weight of each item, $u^{(i)} = rand(0,1)$ is a random number for each item. The probability density of sample point $\boldsymbol{V_t}^{(i)}$ is written as $f(\boldsymbol{V_t}^{(i)})$. On this basis, the sample points can be sorted according to the characteristic value from large to small. And the top M sample points are selected as the experimental points. In addition, the empirical facts suggest the number of initial samples could be small (e.g. $s = 10$), which is sufficient. These s initial sample points are denoted as:

$$S_{ini} = \left\{\boldsymbol{V_t}^{(i)} | i = 1, 2, \dots, s\right\} \tag{18}$$

3.2.2 DNN surrogate model

Both deep neural networks and shallow neural networks can be used to handle the reliability analysis problems. But the DNN model usually possesses a better ability to learn the complex mapping relationship between inputs and system responses than traditional neural networks with single hidden layer [38]. In this work, a reliability analysis framework based on the DNN model is proposed to deal with possible high

nonlinearity problems, which may not be solved by shallow neural networks.

For the ith sample point in the training set, η_i represents the responses of the time-dependent limit function corresponding to the transformed inputs, which can be calculated as

$$\eta_i = g(\boldsymbol{X}^{(i)}, \boldsymbol{Y}^{(i)}, \boldsymbol{S'}^{(i)}, \boldsymbol{I'}^{(i)}, t'^{(i)}) = g(\boldsymbol{V_t}^{(i)}) \tag{19}$$

Based on Eqs. (18)-(19), the input-output training sample points can be collected. With the collected training sample points, the DNN model can be trained. The DNN model transforms the feature representation of the sample from the original space to a new feature space to make classification or prediction easier. As shown in Fig. 2, the DNN model consists of the input layer, output layer, and several hidden layers. In the DNN model, the output of the ith layer is computed as

$$\boldsymbol{h}_i = f_{ac}(\boldsymbol{W}_i \boldsymbol{h}_{i-1} + \boldsymbol{b}_i), \forall i \in \{1, 2, \dots, T\} \tag{20}$$

where $\boldsymbol{h}_i = (h_i^1, \dots, h_i^{d_i})$ are the variables in the ith layer and d_i is the dimension of the ith layer. To be specific, $\boldsymbol{h}_0$ represents the input variables $\boldsymbol{V_t}$ while $\boldsymbol{h}_T$ stands for the prediction output $\hat{\eta}$. Furthermore, the dimension $d_0 = d$ and $d_T = 1$. $\boldsymbol{W}_i \in \mathbb{R}^{d_i \times d_{i-1}}$ and $\boldsymbol{b}_i \in \mathbb{R}^{d_i}$ represent the weight matrix and the vector of bias in the ith hidden layer, respectively. The options of the activation function $f_{ac}(\cdot)$ are usually diverse, which includes the sigmoid function, the hyperbolic tangent function and so on. In this work, the rectified linear unit (ReLU) activation function, expressed as $f_{ac}(h) = \max(0, h)$, is adopted.

Note the network architecture can be decided by the number of hidden layers and the dimension of each hidden layer, i.e., $H = \{T-1, \{d_i\}_{i=1}^{T-1}\}$, which are called as the hyperparameters. A concept that is easily confused with hyperparameters is called as parameters, which are composed of both the weight matrices and the bias vectors in all layers, i.e., $\theta = \{\boldsymbol{W}_i, \boldsymbol{b}_i\}_{i=1}^{T}$. Apparently, the fully H determines the size of θ. As we all known, optimizing the selection of H to determine the optimal network structure is a computationally expensive task. Therefore, generally speaking, the training process of

DNN model only involves the optimization of θ. H is predefined according to empirical knowledge and θ can be determined by minimizing the loss function during the training process. In this work, H is decided by manual tuning and the mean square error (MSE) is adopted as the loss function. The optimization algorithm called Adam [39] is utilized for updating and determining θ of the DNN model. Furthermore, the number of training epochs is 500 and the learning rate is 0.01. Once the initial DNN model is available, the next concern is to select the most suitable new training sample points based on the proposed learning function.

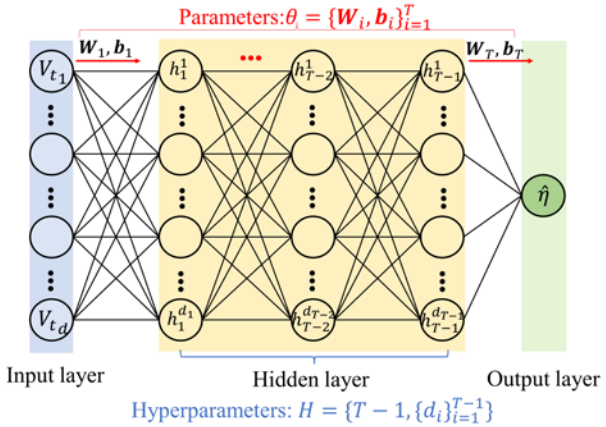

Fig. 2 The construction of the DNN model

3.2.3 The learning function

For active learning methods, one of main concerns is to determine the locations of new selected training sample points at each iteration by the learning function. In general, the most suitable sample points can be selected from two perspectives. First, the selected sample points should be as close to the limit state functions as possible, which contributes the most to the probability of failure. Second, the selected sample points should have higher prediction uncertainty, also called prediction variance. The prediction uncertainty has different representations depending on the constructed surrogate model. In addition, the learning function should also consider that the most suitable new training sample points cannot be too close to the existing training sample points to avoid possible redundant information and ill-conditioned problem.

Similar to the algorithm proposed by Shi et al. [25] for RBF model, we extend the

learning function to system reliability problems for DNN model. Different from the stopping criterion in the reference [25], the average training effect over multiple iterations is considered to ensure that the model gradually converges and stops training rather than by accident. The details about the learning function are listed as following:

Step 1: Rewrite the existing training sample points and then construct DNN model based on them. According to the principle of k cross-validation, the existing training sample points are divided into k subsets. In this work, $k = 5$.The cross-validation samples are obtained where one of the subsets is omitted, which can be expressed as

$$\Omega_{cv}^{(-l)} = ((\boldsymbol{V_t}^{s_1}, \boldsymbol{\eta}^{s_1}), \dots, (\boldsymbol{V_t}^{s_{l-1}}, \boldsymbol{\eta}^{s_{l-1}}), (\boldsymbol{V_t}^{s_{l+1}}, \boldsymbol{\eta}^{s_{l+1}}), \dots (\boldsymbol{V_t}^{s_k}, \boldsymbol{\eta}^{s_k})) \tag{21}$$

where $l = 1,2, \dots k$. Based on each $\Omega_{cv}^{(-l)}$, a DNN model $\hat{g}^{(-l)}(\cdot)$ can be established. By combining the DNN model $\hat{g}(\cdot)$ established by all training samples, a total number of $k + 1$ DNN models are constructed.

Step 2: Estimate the prediction uncertainty of the selected new training sample point defined as $us(\boldsymbol{V_t}^i)$,which can be calculated as

$$us(\boldsymbol{V_t}^i) = \frac{\left|\hat{g}(\boldsymbol{V_t}^i)\right|}{\sqrt{\sum_{l=1}^{k}(\hat{g}^{(-l)}(\boldsymbol{V_t}^i) - \hat{g}(\boldsymbol{V_t}^i))^2/k}} \tag{22}$$

Step 3: Calculate the Euclidean-distance between the selected new training sample point and the existing sample points denoted by $d(\boldsymbol{V_t}^i)$, which can be expressed as

$$d(\boldsymbol{V_t}^i) = \min_{j \in [1,n]} \left\| \boldsymbol{V_t}^i - \boldsymbol{V_t}^j \right\| \tag{23}$$

where $\boldsymbol{V_t}^j$ is the coordinate of the existing training samples.

Step 4: Calculate the active learning function $SLF(\boldsymbol{V_t}^i)$ and choose the most suitable new training sample point. $SLF(\boldsymbol{V_t}^i)$ consider a balance between $us(\boldsymbol{V_t}^i)$ and $d(\boldsymbol{V_t}^i)$, which can be written as

$$SLF(\boldsymbol{V_t}^i) = \frac{(N(us(\boldsymbol{V_t}^i)))^{\beta}}{(N(d(\boldsymbol{V_t}^i)))^{1-\beta}} \tag{24}$$

where $N(\cdot)$ means the normalization operation, which is used to eliminate the effects of different orders of magnitude. For more details about normalization can refer to [25].

At each iteration, the candidate sample point which minimizes the criterion in Eq. (24) is selected as the most suitable new training sample point.

By incorporating the new observations, a new DNN model can be trained. The updating mechanism is performed repeatedly till the predicted failure probability satisfies a predefined stopping criterion, which can be defined as

$$e_s = \frac{3\hat{\sigma}_f}{\bar{\hat{P}}_f} \leq \varepsilon_{th} \tag{25}$$

$$\hat{\sigma}_f = \sqrt{\frac{1}{k}\sum_{i=K-(k-1)}^{K}\left(\bar{\hat{P}}_f - \hat{P}_{fi}\right)^2} \tag{26}$$

$$\bar{\hat{P}}_f = \frac{1}{k}\sum_{i=K-(k-1)}^{K}\hat{P}_{fi} \tag{27}$$

where K represents the Kth iteration process, $\hat{P}_{fi}$ is the predicted failure probability based on the trained DNN model after ith iteration and ε_{th} is a small positive number that can be set by user. In this work, ε_{th} is selected as 0.01.

3.3 Hybrid time-dependent reliability approximation

The main steps of employing the proposed reliability analysis method for HTR-ip are illustrated in Fig. 3.

Step1: Generate N_{mc} Monte Carlo sample points in the design space based on the distribution of the input variables, refer as S_{MCS}.

Step2: Construct instantaneous reliability model using the proposed EUT method.

Step3: Initialize the number of iterations $K = 1$ and generate N_{mc} samples according to transformed uncertain variables, refer as S_{MCS}^{T}.

Step4: Find the candidate experimental points S^c from the candidate pool S^* by using the trained DNN model in the previous iteration if $K > 1$, otherwise skip to the next step. The procedure of selecting the candidate experimental points is as follow: sort the absolute prediction values from small to large by using the DNN trained in the $(K-1)$th iteration and then select first N_{S^c} items. N_{S^c} represents the population size of the candidate experimental points, which is defined as $N_{S^c} = 0.1 * size(S^*)$.

Step5: Select M experiment points from S^c by weighted sampling, refer as S^e. In the first iteration, define the training set S^t from S_{MCS}^{T} with weighted sampling and the

remaining points in S_{MCS}^{T} are referred as the candidate pool S^{*}.

Step6: Update the candidate pool $S^{*} = S^{*} - V_{tnew}$ and the training set $S^{t} = S^{t} + V_{tnew}$ if $K > 1$, otherwise skip to the next step.

Step7: Construct and update the DNN model by using training set S^{t}.

Step8: Predict the failure probability of instantaneous reliability model with samples S_{MCS}^{T} by utilizing DNN model and calculate the stopping criterions. If the values of failure probability do not satisfy the stopping criterion, the process goes to step 9; otherwise, the process goes to step 10.

Step9: Identify the new training sample V_{tnew} with the learning function at set S^{e} and $K = K + 1$. Afterwards, the process goes to step 4.

Step10: Calculate the failure probability for HTR-ip with samples S_{MCS} using the well-trained DNN model.

Step11: Check the coefficient of variation of failure probability $COV(P_f^{min})$. If the value meets the demand, output the probability of failure. Otherwise, the algorithm will go back to step 1 and the size of the Monte Carlo population S_{MCS} should be increased.

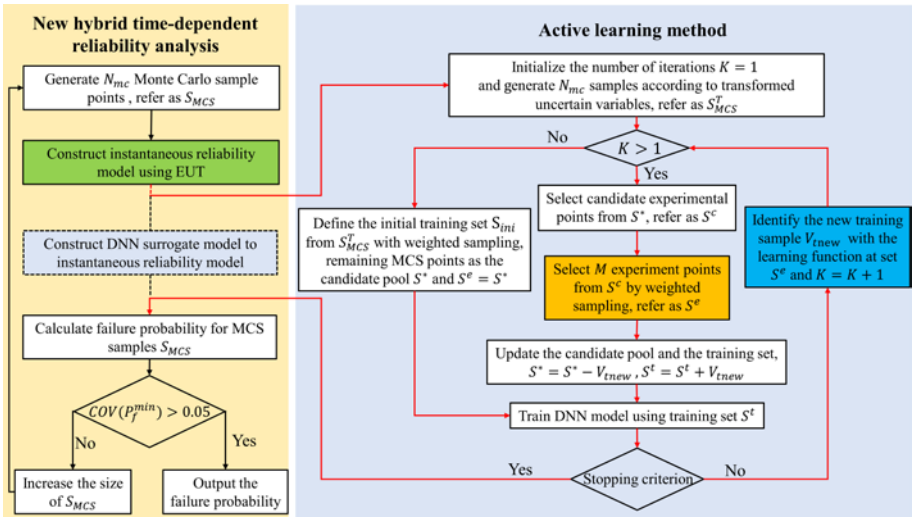

Fig. 3 Flowchart of the proposed reliability analysis method for HTR-ip

4. Numerical example and analysis

In this section, three examples are considered to verify the effectiveness of the proposed approach. The execution time of three examples are also provided. Moreover,

all methods except the direct MCS method were repeated 20 times to verify the stability of performance, and the direct MCS method is repeated 30 times. All the simulation are carried out by using MATLAB R2020a on a 2.90GHz Intel(R) Core(TM) CPU i5-10400.

4.1 Example 1: A math example

In the first example, a mathematical case is studied. The limit state function is formulated as

$$g(X,Y,S(t),I(t),t) = X^2Y - 5X\big(1+S(t)\big)t + (Y+1)t^2 + 5I(t) - 20 \quad (28)$$

where X is a random variable which follows $X \sim N(3.5, 0.25^2)$. Y is an interval variable, and $Y \in [2.5,4.5]$. t is the time parameter and varies in interval $[0,1]$. Additionally, $S(t)$ is a stationary Gaussian process with 0 mean and 1 standard deviation, whose correlation function is defined as Eq. (29). $I(t)$ is a stationary interval process with 0 middle point and 1 radius, whose correlation function are expressed as Eq. (30). The time interval $[0,1]$ for this example is discretized into 200 time instants evenly. Furthermore, the interval variable Y is also discretized into 200 nodes uniformly. 200 MCS samples of the interval process $I(t)$ are generated according to the sampling approach proposed by Jiang. et al [40]. 10^6 random realizations of the stochastic processes and the random variables are generated for the time-dependent hybrid reliability analysis.

$$\rho_S(t_1,t_2) = \exp(-(t_2-t_1)^2) \quad (29)$$

$$\rho_I(t_1,t_2) = \exp(-|t_1-t_2|/3) \quad (30)$$

The first step of employing the proposed approach is to construct an instantaneous reliability model $g(X,Y,S',I',t')$ according to the characterization of the time-varying parameters. As introduced in Sec. 3.1, t is transformed into a uniformly distributed random variable at interval $[0,1]$. As $S(t)$ is a Gaussian process with zero mean and unit variance, S' is a random variable which follows a standard normal distribution. Additionally, due to $I(t)$ is a stationary interval process, I' is a uniformly distributed random variable at a specific interval. Then, within a space domain defined by the

probabilistic attributes of inputs $V_t = [X, Y, S', I', t']$, 10 initial points are generated using the weighted sampling and then be used for evaluating the function output. Given the initial training data sets, an initial low accuracy DNN model can be constructed. In the DNN model, the hidden layers number of the DNN is set to two. Each layer has 10 neurons. Afterwards, the new training sample $[X_{new}, Y_{new}, S'_{new}, I'_{new}, t'_{new}]$ can be obtained by the proposed active learning method introduced. By updating the DNN model iteratively, the instantaneous failure surface can be accurately obtained for further time-dependent hybrid reliability analysis. Eventually, the hybrid time-dependent responses corresponding to the MCS samples can be calculated based on the well trained DNN model.

For comparison purposes, the WS-DNN and CVRBF-MCS methods combined EUT, are also adopted for solving this example in a similar way. As a reference, a direct MCS is carried out to calculate the probability of failure based on Eqs.(9) and (10). The responses of 10^6 random points need to be calculated at each Y node and $I(t)$ node in all time nodes. All the results are given in Tables 1 and 2. As we can see, the proposed method can achieve the best result for the lower and upper bounds of failure probability over all the time intervals. Compared with other methods, the proposed method has the highest accuracy. For efficiency, the number of function evaluations (NOF) of the proposed method and EUT-CVRBF-MCS are much less than that of EUT-WS-DNN. And the proposed method is more efficient than EUT-CVRBF-MCS. Furthermore, the execution time is also provided in Table 1. Influenced by the cross-validation method and the large candidate point pool, EUT-CVRBF-MCS is the most time-consuming method. EUT-WS-DNN is the fastest method due to its mechanism that multiple sample points can be added in one iteration. It can also be seen that the direct MCS cost the least time because the original limit state function is simple and explicit.

The extreme value distribution of the limit state function within the time interval [0,1] is illustrated in Fig. 4. As shown in Fig. 4, the extreme value distributions of the proposed method, EUT-WS-DNN, and EUT-CVRBF-MCS are not completely accurate

compared with MCS in the whole time interval. Nevertheless, the left tails of the probability density curves obtained by the proposed method are exactly the same with the one obtained by MCS. Because the extreme value distribution is accurately approximated in the region corresponding to negative and near to zero values of the limit state function, the proposed method can achieve an accurate estimation of time-variant reliability. The time-dependent failure probability within the time interval [0,1] is illustrated in Fig. 5, which gives a more detail and intuitive display of the results. In summary, the proposed method shows high accuracy and efficiency in this example.

Table 1 Result of example 4.1

Method	p_f^{min}	p_f^{max}	NOF	$\varepsilon^{min}(\%)$	$\varepsilon^{max}(\%)$	Time
Direct MCS	0.10076	0.64686	$200 \times 200 \times 10^6$	------	------	199.68s
Proposed method	0.10061	0.64763	59.2	0.15	0.12	8765.77s
EUT-WS-DNN	0.09639	0.65886	154.5	4.34	1.86	7600.38s
EUT-CVRBF-MCS	0.07510	0.62569	82.5	25.48	3.27	12810.23s

Table 2 Time-dependent probability of failure of example 4.1

Time interval	Direct MCS ([min, max])	Proposed method ([min, max])	EUT-WS-DNN ([min, max])	EUT-CVRBF-MCS ([min, max])
[0,0.2]	[0.00000, 0.10822]	[0.00000, 0.10990]	[0.00000, 0.10773]	[0.00000, 0.12918]
[0,0.4]	[0.00003, 0.34480]	[0.00003, 0.34939]	[0.00003, 0.34335]	[0.00001, 0.34873]
[0,0.6]	[0.00943, 0.49554]	[0.00938, 0.49853]	[0.00949, 0.49487]	[0.00648, 0.50914]
[0,0.8]	[0.04312, 0.58080]	[0.04288, 0.58074]	[0.04338, 0.58191]	[0.03799, 0.58985]
[0,1.0]	[0.10076, 0.64686]	[0.10061, 0.64763]	[0.09639, 0.65886]	[0.07510, 0.625659]

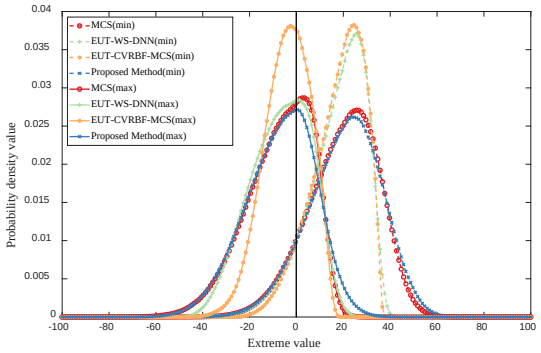

Fig. 4 Extreme value distributions of example 4.1

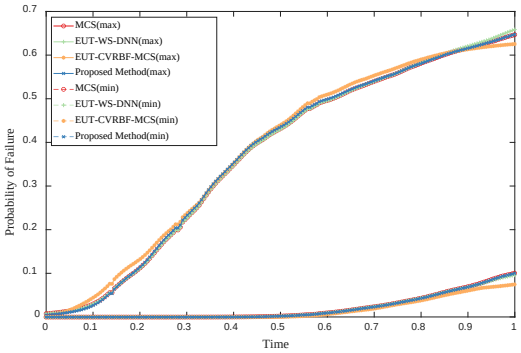

Fig. 5 Time-dependent failure of probability of example 4.1

4.2 Example 2: A Corroded Beam Problem

Here a beam corrosion problem is considered, where the geometry of the beam is shown in Fig. 6. Due to the corrosion, the size of cross section decreases with time.

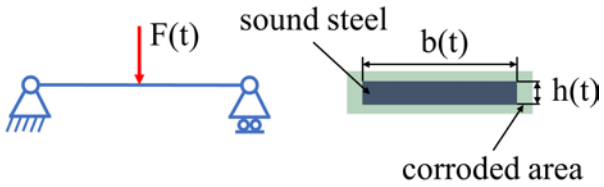

Fig. 6 Corroded beam under midspan load

The beam height $h(t)$ (m) and the beam breadth $b(t)$ (m) are modeled as two time-dependent interval process variables. A stochastic load $F(t)$ (kN) is applied onto the middle point of the beam, which follows a non-stationary process. Its mean function $\mu_F(t)$, standard deviation function $\sigma_F(t)$, and autocorrelation function $p_F(t)$ can be expressed as

$$\mu_F(t) = 800\sin(1.3 + 0.01\mathrm{t}) + 5000 \tag{31}$$

$$\sigma_F(t) = 100\cos(0.04t) + 700 \tag{32}$$

$$p_F(t_1, t_2) = \exp(-(t_2 - t_1)^2) \tag{33}$$

Considering the uncertainty in material properties and manufacturing errors, the yield strength of the material σ (MPa) and the length of corroded beam L (m) are treated as random variables that follow normal distributions, where $\sigma \sim N(200, 20^2)$ and $L \sim N(8.5, 0.2^2)$. The material mass density ρ (kN/m^3) is assumed to an interval

variable. According to the strict mechanical analysis and mathematical treatment, the failure event occurs when the maximum stress exceeds the yielding limit of the beam, and the limit state function associated with the failure is expressed as

$$G\left(\sigma, L, \rho, b(t), h(t), F(t)\right) = \frac{b(t)h(t)^2}{4}\sigma - \left(\frac{F(t)L}{4} + \frac{\rho b(t)h(t)L^2}{8}\right) \tag{34}$$

In this case, two random variables, one stochastic process, one interval variable and two interval processes are involved in the time-dependent limit state function. The distribution parameters of the input interval parameters are summarized in Table 3.

Table 3 Distribution parameters of the input interval parameters

Variable	Type	Midpoint function	Radius function
$b(t)$ (m)	Non-stationary interval process	$0.3 - 5 \times 10^4 t$	0.015
$h(t)$ (m)	Non-stationary interval process	$0.05 - 4 \times 10^4 t$	0.004
ρ (kN/m^3)	Interval variable	78	0.5

And the autocorrelation function of the interval process is given as

$$p_b(t_1, t_2) = p_h(t_1, t_2) = \exp(-|t_1 - t_2|/3) \tag{35}$$

In this example, the considered time period is given as [1, 30] month, which is evenly discretized into 59 time nodes. For the MCS samples of this example, 10^6 samples are generated according to the probability distribution of random uncertainty parameters, and 200 samples are generated according to interval uncertainty parameters. The proposed approach is employed to solve the corroded beam problem. By performing proposed EUT approach, the stochastic process variables and the interval process variables can be represented as a random variable characterized by a specific probability distribution. Taking the beam breadth $b(t)$ as an example, the PDF of the translated random variable b' is obtained by the average of the PDFs of the interval process $b(t)$ over time period [1, 30]. Fig. 7 shows the approximated PDFs of b' and the interval process $b(t)$ with $t = [1, 10, 20, 30]$ respectively. Then, an instantaneous reliability model formulated as $G(\sigma, L, \rho, b', h', F')$ can be constructed, which can cover all the potential instantaneous failure events that may occur in hybrid time-

dependent corroded beam system during a specified period of time. With the proposed active learning method, the DNN model is capable of approximating the instantaneous reliability model accurately while reducing vast computational resources. In the DNN model, the hidden layer number of the DNN is set to two and each layer has 15 neurons. Afterwards, the hybrid time-dependent reliability analysis can be obtained based on the obtained high-precision DNN model and the MCS samples.

As a comparison, two existing active learning methods, WS-DNN and CVRBF-MCS method combined EUT, are also utilized to solve this example in a similar way. As a reference, a direct MCS is carried out to calculate the probability of failure by evaluating the responses of MCS samples at all times. All the results are given in Tables 4 and 5. As show in Table 5, the proposed method is more accurate than the other two methods. According to the extreme value distribution illustrated in Fig. 8, the left tails of the probability density curve obtained by the proposed method are also more accurate than the other two methods and exactly the same with the one obtained by MCS. EUT-WS-DNN method performs the worst over all the time intervals. This phenomenon can be more intuitively reflected in Fig. 9. The execution time is provided in Table 4. The execution time required by the proposed method is much less than that of other two active learning methods. It also can be seen in Table 4 that the NOF of the proposed method is much less than that of EUT-WS-DNN and EUT-CVRBF-MCS, and the EUT-WS-DNN method also performs the worst in terms of efficiency. The fundamental reason is that the response range of the corroded beam structure is wide and the proportion of sample points near the failure surface is small. So, it is difficult to manually set an appropriate threshold method to ensure the accuracy and efficiency of the EUT-WS-DNN method. This further illustrates the importance of the proposed active learning method for the surrogate model approach in reliability analysis. To sum up, all of the results indicate that the proposed method performs well in terms of accuracy and efficiency in this beam corrosion problem.

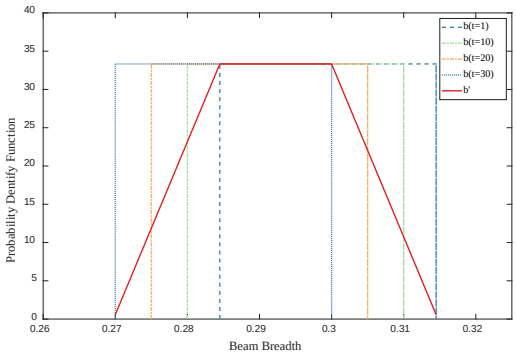

Fig. 7 Translation of the interval process $b(t)$

Table 4 Result of example 4.2

Method	p_f^{min}	p_f^{max}	NOF	$\varepsilon^{min}(\%)$	$\varepsilon^{max}(\%)$	Time
Direct MCS	0.23353	0.91977	$59 \times 200 \times 10^6$	------	------	115.62s
Proposed method	0.24374	0.91786	36.2	4.37	0.21	1856.66s
EUT-WS-DNN	0.25781	0.91815	216.0	10.40	0.18	3562.92s
EUT-CVRBF-MCS	0.20489	0.89079	104.5	12.26	3.15	9573.49s

Table 5 Time-dependent probability of failure of example 4.2

Time interval	Direct MCS ([min, max])	Proposed method ([min, max])	EUT-WS-DNN ([min, max])	EUT-CVRBF-MCS ([min, max])
[1,6]	[0.00053, 0.02235]	[0.00052, 0.02103]	[0.00000, 0.02106]	[0.00003, 0.02149]
[1,12]	[0.00301, 0.08958]	[0.00298, 0.09084]	[0.00003, 0.13564]	[0.00137, 0.08432]
[1,18]	[0.01825, 0.31897]	[0.01599, 0.32448]	[0.00339, 0.37614]	[0.01569, 0.30897]
[1,24]	[0.07034, 0.65819]	[0.07073, 0.65799]	[0.05849, 0.71819]	[0.05813, 0.67989]
[1,30]	[0.23353, 0.91977]	[0.24374, 0.91786]	[0.25781, 0.91815]	[0.20489, 0.89079]

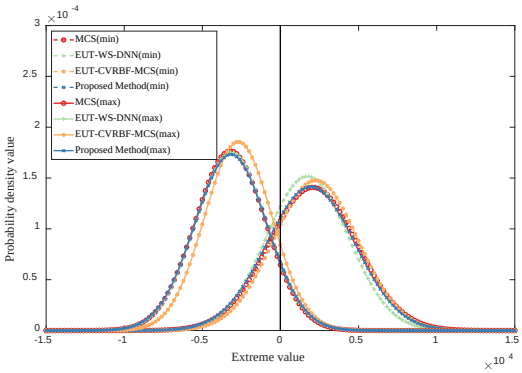

Fig. 8 Extreme value distributions of example 4.2

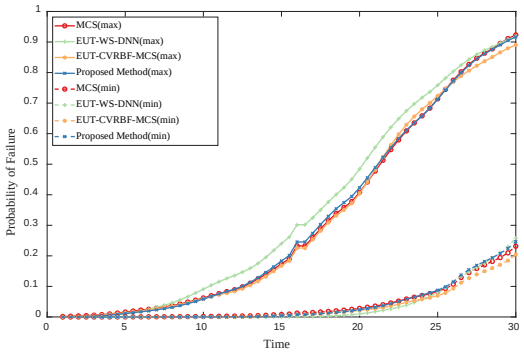

Fig. 9 Time-dependent failure of probability of example 4.2

4.3 Example 3: A phononic crystal problem

Phononic crystals are periodic composites with the band gap of elastic waves, where the structure of the 2-Dimension phononic crystal is shown in Fig. 10. They can prevent elastic waves of selected ranges of frequencies from being transmitted through the material. Theoretically, the elastic waves whose frequencies located within the band gap are prohibited to transmit. Reliable inhibition of a specific frequency needs to be achieved during the early design stages of phononic crystals. Therefore, it is of great importance to analyze the reliability of the designed phononic crystals.

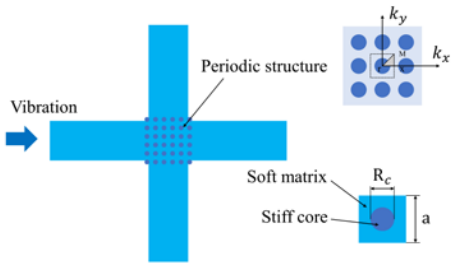

Fig. 10 The structure of 2-Dimension phononic crystal

Due to manufacturing error and material aging, the sizes and the material parameters of the 2-D phononic crystal have significant effect on the property of the phononic crystals. All of the uncertainty parameters about the sizes and the material properties are given in Table 6. And $a(t)$ (m) represents the width of soft matrix, E(GPa), $\rho(\mathrm{kN/m^3})$, and ν represent the Young's modulus, the material density, and the Poisson's ratio, respectively, and $R_c(t)$ (m) stands for the diameter of stiff core. The correlation functions of stochastic processes and interval processes are also defined as

Eq. (33) and Eq. (35), respectively. Usually, it is difficult but important for phononic crystals to attenuate low-frequency elastic waves. Here, the structure failure occurs if the lower bound of the first band gap within the time interval yields a threshold 268 Hz. The unit cell of phononic crystals is discretized into triangular elements. The number of elements is 179 and the number of nodes is 316. The band gap is obtained by performing the eigenfrequency analysis and parametric sweep in the COMSOL acoustic module. And the limit state function of the phononic crystal can be formulated as

$$G(\boldsymbol{V_o}) = 268 - \delta_{FEM\_lb1}(\boldsymbol{V_o}) \tag{36}$$

where the function $\delta_{FEM\_lb1}(\cdot)$ represents the lower bound of the first band gap evaluated by the FEM and $\boldsymbol{V_o}$ denotes the uncertainty input parameters. Due to the calculation of this example is highly time-consuming, only 200 samples are generated according to the probability distribution of random uncertainty variables, and 10 samples are generated according to interval uncertainty variables. In this study, the time interval [1, 5] is evenly discretized into 5 time nodes.

The proposed approach is employed for hybrid time-dependent reliability analysis of the phononic crystal. The hidden layer number of the DNN and the widths of the hidden layers are set to 3 and 12, respectively. To validate the accuracy of the proposed method, the predicted failure of probability is compared with direct MCS, EUT-WS-DNN and EUT-CVRBF-MCS. As shown in Fig. 11, more accurate hybrid time-dependent reliability analysis can be achieved by utilizing the proposed method than the other two methods. The reason is that the failure of probability of instantaneous reliability model after conducting equivalent uncertainty transformation is small. The proposed method has higher precision due to the weighted sampling method ensure that failure points exist as much as possible in candidate experimental points and the learning function can find experimental points near LSS more accurately. To investigate the efficiency of the proposed method, the NOF and the execution time of all methods are given in Tables 7. It is clear that the proposed method is more efficiency compared with other two active learning methods. With 112.3 function evaluations, the proposed

method provides an accurate reliability estimation with $\varepsilon^{min} = 0$ and $\varepsilon^{max} = 3.57\%$, while other two methods have lower accuracy. The results demonstrate that the proposed method is applicable to hybrid time-dependent reliability analysis of phononic crystal.

Table 6 Distribution parameters of the input uncertainty parameters

Variable	Type	Mean function or Midpoint function	Standard deviation function or Radius function
$a(t)$ (m)	Non-stationary stochastic process	$e^{-1000t}\sin(1.3+0.01t)+0.02$	$e^{-1000t}\cos(0.04t)+0.0005$
E_1 (GPa)	Random variable	1.175	0.05
E_2 (GPa)	Random variable	4.08	0.2
ρ_1 (kN/m^3)	Random variable	1300	130
ρ_2 (kN/m^3)	Random variable	11600	100
ν_1	Interval variable	0.46885	0.0005
ν_2	Interval variable	0.3791	0.01
$R_c(t)$ (m)	Non-stationary interval process	$0.008-0.0001t$	$0.0002\sin(0.5\pi+0.01t)$

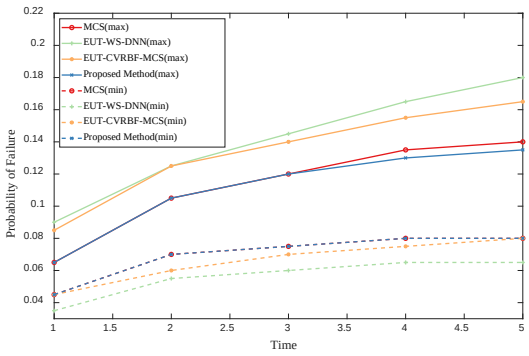

Fig. 11 Time-dependent failure of probability of example 4.3

Table 7 Result of example 4.3

Method	p_f^{min}	p_f^{max}	NOF	ε^{min}(%)	ε^{max}(%)	Time
Direct MCS	0.0800	0.1400	$5\times10\times200$	------	------	>89h
Proposed method	0.0800	0.1350	112.3	0	3.57	3939.51s
EUT-WS-DNN	0.0650	0.1800	2232.5	18.75	28.57	73056.25s
EUT-CVRBF-MCS	0.0800	0.1650	156.7	0	17.86	5592.75s

5. Conclusion

In this paper, a new hybrid time-dependent reliability analysis model involving interval processes, termed as HTR-ip, is developed for practical engineered system with limited data over the life cycle. For efficiently estimating the developed HTR-ip, an equivalent uncertainty transformation approach is presented for considering both random process and interval process. By translating the random processes and interval processes into equivalent random variables, an instantaneous reliability model is constructed to envelope all potential system failures during the time interval. In order to further improve the efficiency and accurately identify the instantaneous failure surface, an active learning method is proposed by combining the DNN model and the weighted sampling method. Instead of the actual physical model, the new hybrid time-dependent reliability can be obtained by the Monte Carlo simulations based on the well trained DNN model.

Numerical results demonstrate that the proposed method can achieve high accuracy and efficiency for the HTR-ip problems. Though the direct MCS is more efficient than the proposed method when the limit state function is explicit. However, the limit state function is usually implicit in engineering problem, which requires a time-consuming numerical calculation of the structural response by mean of finite element analysis. As a consequence, the proposed method is more suitable and competitive compared with direct MCS.

This study provides a meaningful supplement for the traditional hybrid static reliability analysis. Furthermore, the proposed active learning method also has good application potential in other surrogate model methods for reliability analysis problems.

Acknowledgement

The paper is supported by the National Natural Science Foundation of China (Grant No. 51905162), the Foundation for Innovative Research Groups of the National Natural Science Foundation of China (Grant No. 51621004) and the Natural Science

Foundation of Hunan Province (Grant No. 2022JJ30132). The author would also like to thank reviewers for their valuable suggestions.

References

[1] M. Faes, D. Moens, Recent trends in the modeling and quantification of non-probabilistic uncertainty, Archives of Computational Methods in Engineering, 27 (2020) 633-671.
[2] Z. Zheng, H. Dai, Y. Wang, W. Wang, A sample-based iterative scheme for simulating non-stationary non-Gaussian stochastic processes, Mechanical Systems and Signal Processing, 151 (2021) 107420.
[3] M. Shields, G. Deodatis, Estimation of evolutionary spectra for simulation of non-stationary and non-Gaussian stochastic processes, Computers & Structures, 126 (2013) 149-163.
[4] A. Balu, B. Rao, Inverse structural reliability analysis under mixed uncertainties using high dimensional model representation and fast Fourier transform, Engineering structures, 37 (2012) 224-234.
[5] C. Eckert, M. Beer, P.D. Spanos, A polynomial chaos method for arbitrary random inputs using B-splines, Probabilistic Engineering Mechanics, 60 (2020) 103051.
[6] G. Li, Z. Lu, J. Xu, A fuzzy reliability approach for structures based on the probability perspective, Structural Safety, 54 (2015) 10-18.
[7] P. Wei, J. Song, S. Bi, M. Broggi, M. Beer, Z. Lu, Z. Yue, Non-intrusive stochastic analysis with parameterized imprecise probability models: I. Performance estimation, Mechanical Systems and Signal Processing, 124 (2019) 349-368.
[8] Y. Song, J. Mi, Y. Cheng, L. Bai, K. Chen, A dependency bounds analysis method for reliability assessment of complex system with hybrid uncertainty, Reliability Engineering & System Safety, 204 (2020) 107119.
[9] F. Li, Z. Luo, J. Rong, N. Zhang, Interval multi-objective optimisation of structures using adaptive Kriging approximations, Computers & Structures, 119 (2013) 68-84.
[10] M. Di Paola, L. Galuppi, G.R. Carfagni, Fractional viscoelastic characterization of laminated glass beams under time-varying loading, International Journal of Mechanical Sciences, 196 (2021) 106274.
[11] C. Bucher, A. Di Matteo, M. Di Paola, A. Pirrotta, First-passage problem for nonlinear systems under Lévy white noise through path integral method, Nonlinear Dynamics, 85 (2016) 1445-1456.
[12] C. Wang, M. Beer, B.M. Ayyub, Time-Dependent Reliability of Aging Structures: Overview of Assessment Methods, ASCE-ASME Journal of Risk and Uncertainty in Engineering Systems, Part A: Civil Engineering, 7 (2021) 03121003.
[13] C. Andrieu-Renaud, B. Sudret, M. Lemaire, The PHI2 method: a way to compute time-variant reliability, Reliability Engineering & System Safety, 84 (2004) 75-86.
[14] Z. Hu, X. Du, Time-dependent reliability analysis with joint upcrossing rates, Structural and Multidisciplinary Optimization, 48 (2013) 893-907.

[15] J. Xu, F. Kong, An adaptive cubature formula for efficient reliability assessment of nonlinear structural dynamic systems, Mechanical Systems and Signal Processing, 104 (2018) 449-464.
[16] T. Crestaux, O. Le Maıtre, J.-M. Martinez, Polynomial chaos expansion for sensitivity analysis, Reliability Engineering & System Safety, 94 (2009) 1161-1172.
[17] B. Sudret, Global sensitivity analysis using polynomial chaos expansions, Reliability engineering & system safety, 93 (2008) 964-979.
[18] B. Gaspar, A.P. Teixeira, C.G. Soares, Assessment of the efficiency of Kriging surrogate models for structural reliability analysis, Probabilistic Engineering Mechanics, 37 (2014) 24-34.
[19] Z. Wang, P. Wang, A new approach for reliability analysis with time-variant performance characteristics, Reliability Engineering & System Safety, 115 (2013) 70-81.
[20] L. Hong, H. Li, J. Fu, J. Li, K. Peng, Hybrid active learning method for non-probabilistic reliability analysis with multi-super-ellipsoidal model, Reliability Engineering & System Safety, 222 (2022) 108414.
[21] A.A. Chojaczyk, A.P. Teixeira, L.C. Neves, J.B. Cardoso, C.G. Soares, Review and application of artificial neural networks models in reliability analysis of steel structures, Structural Safety, 52 (2015) 78-89.
[22] Y. Bao, Z. Xiang, H. Li, Adaptive subset searching-based deep neural network method for structural reliability analysis, Reliability Engineering & System Safety, 213 (2021) 107778.
[23] W.J.d.S. Gomes, Shallow and deep artificial neural networks for structural reliability analysis, ASCE-ASME J Risk and Uncert in Engrg Sys Part B Mech Engrg, 6 (2020).
[24] Z. Xiang, J. Chen, Y. Bao, H. Li, An active learning method combining deep neural network and weighted sampling for structural reliability analysis, Mechanical Systems and Signal Processing, 140 (2020) 106684.
[25] L. Shi, B. Sun, D.S. Ibrahim, An active learning reliability method with multiple kernel functions based on radial basis function, Structural and Multidisciplinary Optimization, 60 (2019) 211-229.
[26] L. Wang, X. Wang, X. Chen, R. Wang, Time-variant reliability model and its measure index of structures based on a non-probabilistic interval process, Acta Mechanica, 226 (2015) 3221-3241.
[27] C. Jiang, B. Ni, X. Han, Y. Tao, Non-probabilistic convex model process: a new method of time-variant uncertainty analysis and its application to structural dynamic reliability problems, Computer Methods in Applied Mechanics and Engineering, 268 (2014) 656-676.
[28] Q. Chang, C. Zhou, P. Wei, Y. Zhang, Z. Yue, A new non-probabilistic time-dependent reliability model for mechanisms with interval uncertainties, Reliability Engineering & System Safety, 215 (2021) 107771.
[29] L. Wang, Y. Liu, M. Li, Time-dependent reliability-based optimization for

structural-topological configuration design under convex-bounded uncertain modeling, Reliability Engineering & System Safety, 221 (2022) 108361.
[30] N. Chen, S. Xia, D. Yu, J. Liu, M. Beer, Hybrid interval and random analysis for structural-acoustic systems including periodical composites and multi-scale bounded hybrid uncertain parameters, Mechanical Systems and Signal Processing, 115 (2019) 524-544.
[31] J. Chen, Z. Wan, A compatible probabilistic framework for quantification of simultaneous aleatory and epistemic uncertainty of basic parameters of structures by synthesizing the change of measure and change of random variables, Structural Safety, 78 (2019) 76-87.
[32] J. Zhang, M. Xiao, L. Gao, J. Fu, A novel projection outline based active learning method and its combination with Kriging metamodel for hybrid reliability analysis with random and interval variables, Computer Methods in Applied Mechanics and Engineering, 341 (2018) 32-52.
[33] C. Jiang, J. Zheng, X. Han, Probability-interval hybrid uncertainty analysis for structures with both aleatory and epistemic uncertainties: a review, Structural and Multidisciplinary Optimization, 57 (2018) 2485-2502.
[34] D. Wang, C. Jiang, H. Qiu, J. Zhang, L. Gao, Time-dependent reliability analysis through projection outline-based adaptive Kriging, Structural and Multidisciplinary Optimization, 61 (2020) 1453-1472.
[35] Y. Shi, Z. Lu, Dynamic reliability analysis model for structure with both random and interval uncertainties, International Journal of Mechanics and Materials in Design, 15 (2019) 521-537.
[36] Z. Wang, C. Wei, Time-variant reliability assessment through equivalent stochastic process transformation, Reliability Engineering & System Safety, 152 (2016) 166-175.
[37] C. Jiang, G. Lu, X. Han, L. Liu, A new reliability analysis method for uncertain structures with random and interval variables, International Journal of Mechanics and Materials in Design, 8 (2012) 169-182.
[38] Y. Bengio, I. Goodfellow, A. Courville, Deep learning, MIT press Cambridge, MA, USA, 2017.
[39] D.P. Kingma, J. Ba, Adam: A method for stochastic optimization, arXiv preprint arXiv:1412.6980, (2014).
[40] C. Jiang, N. Liu, B. Ni, A Monte Carlo simulation method for non-random vibration analysis, Acta Mechanica, 228 (2017) 2631-2653.